

DISCOVERY OF A 105 MS X-RAY PULSAR IN KESTEVEN 79:
ON THE NATURE OF COMPACT CENTRAL OBJECTS IN SUPERNOVA REMNANTS

E. V. GOTTHELF & J. P. HALPERN

Columbia Astrophysics Laboratory, Columbia University, 550 West 120th Street, New York, NY 10027-6601; eric@astro.columbia.edu,
jules@astro.columbia.edu

AND

F. D. SEWARD

Smithsonian Astrophysical Observatory, 60 Garden Street, Cambridge, MA 02138; fds@head.cfa.harvard.edu

(Accepted March 17, 2005)

Submitted February 14, 2005

ABSTRACT

We report the discovery of 105-ms X-ray pulsations from the compact central object (CCO) in the supernova remnant Kes 79 using data acquired with the *Newton X-Ray Multi-Mirror Mission*. Two observations of the pulsar taken 6 days apart yield an upper limit on its spin-down rate of $\dot{P} < 7 \times 10^{-14} \text{ s s}^{-1}$ and no evidence for binary orbital motion. The implied energy loss rate is $\dot{E} < 2 \times 10^{36} \text{ ergs s}^{-1}$, surface magnetic field strength is $B_p < 3 \times 10^{12} \text{ G}$, and spin-down age is $\tau > 24 \text{ kyr}$. The latter exceeds the remnant's estimated age, suggesting that the pulsar was born spinning near its current period. The X-ray spectrum of PSR J1852+0040 is best characterized by a blackbody model of temperature $kT_{BB} = 0.44 \pm 0.03 \text{ keV}$, radius $R_{BB} \approx 0.9 \text{ km}$, and $L_{bol} = 3.7 \times 10^{33} \text{ ergs s}^{-1}$ at $d = 7.1 \text{ kpc}$. The sinusoidal light curve is modulated with a pulsed fraction of $> 45\%$, suggestive of a small hot spot on the surface of the rotating neutron star. The lack of a discernible pulsar wind nebula is consistent with an interpretation of PSR J1852+0040 as a rotation-powered pulsar whose spin-down luminosity falls below the empirical threshold for generating bright wind nebulae, $\dot{E}_c \approx 4 \times 10^{36} \text{ ergs s}^{-1}$. The age discrepancy implies that its \dot{E} has always been below \dot{E}_c , perhaps a distinguishing property of the CCOs. Alternatively, the X-ray spectrum of PSR J1852+0040 suggests a low-luminosity AXP, but the weak inferred B_p field is incompatible with a magnetar theory of its X-ray luminosity. So far, we cannot exclude accretion from a fall-back disk. The ordinary spin parameters discovered from PSR J1852+0040 highlight the difficulty that existing theories of isolated neutron stars have in explaining the high luminosities and temperatures of CCO thermal X-ray spectra. *Subject headings:* stars: neutron — pulsars: (CXOU J185238.6+004020, PSR J1852+0040) — supernova remnants: individual (Kes 79)

1. INTRODUCTION

The discovery in recent years of many isolated neutron stars (NSs) at the centers of supernova remnants (SNRs) confirms the long-held notion that these ultra-dense stellar remnants are born in supernova explosions (Baade & Zwicky 1934). Most of these NSs are identified as pulsars, whose emission derives either from rotational energy loss, as for the rapidly spinning pulsars in the Crab ($P = 33 \text{ ms}$) and Vela ($P = 89 \text{ ms}$) remnants, or from magnetic field decay, as posited for the slower ($5 < P \leq 12 \text{ s}$) anomalous X-ray pulsars (AXPs) and related objects (see Mereghetti 2000 for a review). However, the nature of a small but growing collection of young ($\lesssim 10^4 \text{ yrs}$) NSs in SNRs remains a mystery. These so-called Compact Central Objects (CCOs) are seemingly isolated NSs, distinguished by their steady flux, predominantly thermal emission, lack of optical or radio counterparts, and absence of a surrounding pulsar wind nebula (see Pavlov, Sanwal, & Teter 2004 for a review).

The six firm examples of CCOs are the central X-ray sources discovered in Cas A (Tananbaum 1999), Pup A (Petre, Becker, & Winkler 1982), G347.3–0.5 (Slane et al. 1999), PKS 1209–51/52 (Helfand & Becker 1984), G266.2–1.2 (Slane et al. 2001), and Kes 79 (Seward et al. 2003). Their luminosities range over

$10^{33} \lesssim L_x \lesssim 10^{34} \text{ erg s}^{-1}$, typical of the younger pulsars; however their spectra are best characterized as hot blackbody emission of $kT_{BB} \sim 0.4 \text{ keV}$, rather than by power-law models. This is significantly hotter than radio pulsars or other radio-quiet NSs (RQNSs; e.g., Caraveo, Bignami, & Trümper 1996), but similar to the thermal component of the more luminous AXPs/SGRs. Distinct from the rest, PSR J1210–5226 in PKS 1209–51/52 is a 424 ms pulsar (Zavlin et al. 2000) that displays large deviations in its spin-down rate, a softer spectrum of $kT_{BB} = 0.22 \text{ keV}$, and cyclotron resonance lines (Sanwal et al. 2002; Pavlov et al. 2002; Mereghetti 2002; Bignami et al. 2003; Zavlin, Pavlov, & Sanwal 2004). These properties suggest that PSR J1210–5226 is variously a wide-binary system, a strongly glitching NS, or an accretor from fall-back material (Zavlin et al. 2004).

CXOU J185238.6+004020 is the recently discovered CCO in supernova remnant Kes 79 (G33.6+0.1; Seward et al. 2003). The distance to this unresolved *Chandra* source is estimated as 7.1 kpc, derived from H I and OH absorption studies (Frail & Clifton 1989; Green & Dewdney 1992) and updated using the Galactic rotation curves of Case & Bhattacharya (1998). Its X-ray luminosity all but rules out any late-type star, and the spectral slope (photon index $\Gamma = 4.2$; Seward et al. 2003) nominally eliminates an AGN origin. The steady

flux disfavors an accreting binary origin for the X-ray emission, and the absence of a wind nebula argues against an energetic rotation-powered pulsar. In this paper we report the discovery of 105 ms pulsations from the CCO associated with Kes 79, with an upper limit on the period derivative, and we consider possible interpretations of its timing and spectral properties. We leave the analysis of the SNR to a subsequent paper.

2. XMM-Newton OBSERVATIONS

The central source in Kes 79 was observed twice with the *Newton X-Ray Multi-Mirror Mission (XMM-Newton)* on 2004 October 18 and 23. We analyze data from the European Photon Imaging Camera (EPIC; Turner et al. 2003), which consists of three CCD imagers, EPIC pn and two EPIC MOSs. These detectors are sensitive to X-rays in the nominal 0.1 – 12 keV range. The EPIC pn was operated in “small window” mode with a $4'3 \times 4'3$ field-of-view (FOV) and 5.7 ms time resolution that allows a search for even the most rapidly rotating pulsar. The target was placed at the default EPIC pn focal plane location for a point source. The EPIC MOS data were obtained in “full frame” mode with a 30' diameter FOV to image the diffuse supernova remnant emission and its environment. The time resolution in this mode is 2.7 s. For all three cameras the medium density filter was used.

We processed the data with Science Analysis System version SAS 6.0.0 (20040318_1831), and screened the photon event lists using the standard filter criteria. Both observations were uncontaminated by flare events and provided 30.5 ks of good EPIC pn exposure time during each epoch. After taking into account the CCD read-out dead-time (29%), this translates to 21.6 ks of live-time per observation in “small window” mode. Each EPIC MOS provided nearly 31 ks of good exposure time per observation with no dead-time. In all cases, the source count rates were too low for pile-up effects to be significant. Photon arrival times were converted to the solar system barycenter using the *Chandra* derived source coordinates, $18^{\text{h}}52^{\text{m}}38^{\text{s}}.57, +00^{\circ}40'19''.8$ (J2000.0), which we determined from the latest aspect analysis.

Figure 1 shows the exposure-corrected EPIC MOS image of Kes 79 incorporating data from both *XMM-Newton* observations, centered on CXOU J185238.6+004020. The new data closely matches the earlier *Chandra* image presented in Sun et al. (2004). In the vicinity of the pulsar the surface brightness of the SNR varies greatly. This requires care in choosing the source and background regions. In the following analysis we choose a small source aperture $30''$ in diameter centered on CXOU J185238.6+004020 to minimize background contamination from the SNR. This region encloses $\geq 80\%$ of the source flux. An annular background region would be contaminated by the increased SNR emission to the northwest of the pulsar. This is particularly troublesome for the spectral analysis since the soft source spectrum overlaps that of the thermal emission from the SNR. Instead, background counts were accumulated from a relatively uniform, $30''$ diameter region centered at coordinates $18^{\text{h}}52^{\text{m}}39^{\text{s}}.30, +00^{\circ}39'49''.2$ (J2000.0), which is just to the southeast of the source.

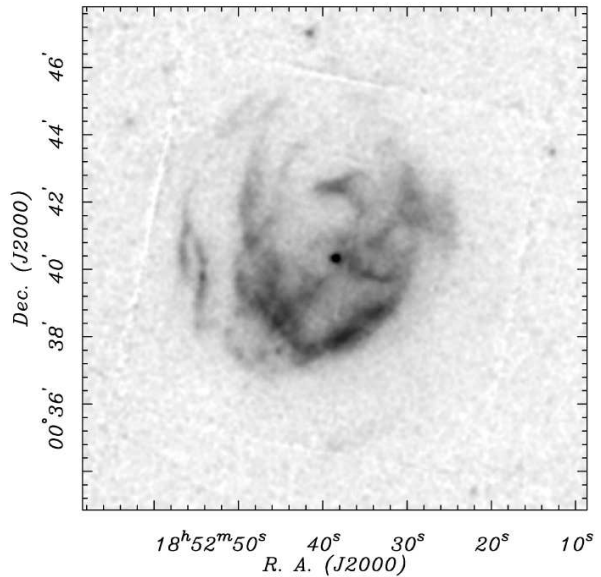


FIG. 1.— The 61.7 ks *XMM-Newton* EPIC MOS exposure-corrected X-ray image (0.3 – 10 keV) of the shell-type supernova remnant Kes 79. The image is smoothed with a 3-pixel boxcar algorithm and scaled by the square-root of the intensity. Gaps between the CCDs are visible as linear artifacts. Timing analysis of the central point-source, CXOU J185238.6+004020, using the EPIC pn data, reveals a 105 ms pulsar.

3. TIMING ANALYSIS

Arrival times of photons in the energy range 0.3 – 10 keV were extracted from the source region and searched for a pulsed signal using the Fast Fourier Transform (FFT) algorithm. A highly significant signal is detected in the October 18 time series at $P = 105$ ms using a 2^{23} -bin transform. No higher harmonics were found. We constructed a periodogram centered on this signal using the Z_1^2 (Rayleigh) test (Buccheri et al. 1983) and localized the pulsed emission to $P = 104.91264(4)$ ms with a peak statistic of $Z_1^2 = 130$, after refining the energy range to an optimal 1 – 5 keV energy band. The number in parenthesis is the 95% confidence uncertainty in the last digit computed using the Monte Carlo method described in Gotthelf, Vasisht, & Dotani (2003). The detection significance corresponds to a negligible probability of chance occurrence. The periodogram is shown in Figure 2 along with the roughly sinusoidal pulse profile folded at the best period. A similar analysis of the 2004 October 23 time series produced a notably weaker signal with $Z_1^2 = 56$ at $P = 104.91261(5)$ ms (see Table 1). In neither observation do we find evidence of significant energy dependence in the pulse shape.

The background-subtracted pulsed fraction is $86 \pm 16\%$ and $61 \pm 16\%$ for the two observations, respectively. Here, we define the pulsed fraction as $f_p \equiv N(\text{pulsed})/N(\text{total})$, where we choose the minimum of the folded light curves as the unpulsed level. The quoted uncertainties are derived by propagating the counting statistics of the light curve, but the pulsed fraction is also quite sensitive to systematic uncertainty in the background, which contributes about half of the total counts. The differences in Z_1^2 and f_p between the two observations are suggestive of a real change, but not large enough to be considered reliable at this stage. According

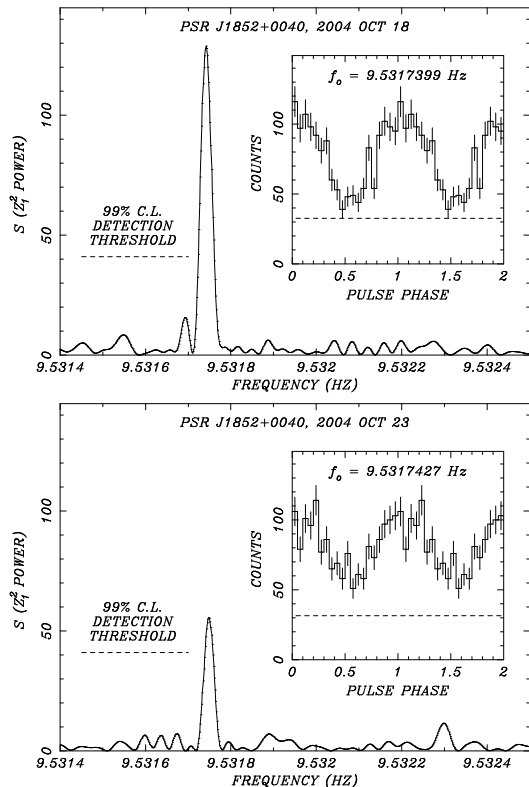


FIG. 2.— Discovery of PSR J1852+0040 in Kes 79 using *XMM-Newton* EPIC pn data acquired on 2004 October 18 (*left*) and October 23 (*right*). A highly significant signal is found in 1 – 5 keV photons extracted from a 30'' diameter aperture at the location of CXOU J185238.6+004020. The detection threshold for a blind search of a 2^{23} -element FFT is indicated. *Inset*: Folded light-curve of PSR J1852+0040. The background level is indicated by the dashed line.

TABLE 1
XMM-Newton TIMING RESULTS FOR PSR J1852+0040

Epoch (MJD[TDB])	Expo (s)	Bkg ^a (s ⁻¹)	Source ^b (s ⁻¹)	Period ^c (s)	f_p ^d (%)
53296.00135994	30587	0.030(1)	0.041(2)	0.10491264(4)	86(16)
53301.98462573	30515	0.029(1)	0.046(2)	0.10491261(5)	61(16)

^aBackground rate obtained using a $r = 0'.25$ aperture placed just southeast of the source region (see §2), and corrected for dead-time. Statistical (\sqrt{N}) uncertainty in the last digit is given in parentheses.

^bBackground and dead-time corrected count rate for a $r = 0'.25$ aperture. Statistical (\sqrt{N}) uncertainty in the last digit is given in parentheses.

^cPeriod derived from a Z_1^2 test. Period uncertainty is 95% confidence computed by the Monte Carlo method described in Gotthelf, Vasisht, & Dotani (2003).

^dPulsed fraction defined as $f_p \equiv N(\text{pulsed})/N(\text{total})$.

to the prescription of Pavlov, Zavlin, & Trümper (1999), the two values of Z_1^2 are inconsistent at approximately the 3σ level. If there is real variability of the pulse shape, it has important implications for the origin of the emission.

The uncertainty on the period measurement from the two *XMM-Newton* observations is too large to derive a significant spin-down rate. In fact, the measured

period *decreased* with time, although not significantly, $\dot{P} = \Delta P/\Delta T = (-6 \pm 13) \times 10^{-14} \text{ s s}^{-1}$. The error range is the 95% confidence interval and is computed by propagating the uncertainties on the individual period measurements. We also searched the combined data set over a plausible range of P and \dot{P} , for increased sensitivity. We were not able to identify the correct period derivative unambiguously from the multiplicity of possible solutions. For an upper limit on the period derivative of $\dot{P} < 7 \times 10^{-14} \text{ s s}^{-1}$ we can constrain the spin-down power of PSR J1852+0040 to $\dot{E} < 2 \times 10^{36} \text{ ergs s}^{-1}$, the inferred magnetic field to $B_p < 3 \times 10^{12} \text{ G}$, and the characteristic age to $\tau \equiv P/2\dot{P} > 24 \text{ kyr}$, parameters that are typical of a rotation-powered pulsar with a normal magnetic field strength.

The two observations of PSR J1852+0040 also allow us to place an upper limit on its radial acceleration over 6 days corresponding to $\Delta v_r < 0.32 \text{ km s}^{-1}$. Finally, we looked for acceleration on 1 – 8 hr timescales by cross-correlating the pulse profiles obtained from sub-sections of the time series with a template profile constructed from all the data. For the first observation, we derive an upper limit of $a_x \sin i < 0.01 \text{ light-seconds}$, less than those found for the AXPs (Mereghetti, Israel, & Stella 1998). The data from the second observation are somewhat less constraining. These limits exclude a main-sequence companion filling its Roche lobe for inclination angles $i > 10^\circ$, the latter having 98.5% a priori probability.

Previous searches for pulsations from the direction of Kes 79 were inconclusive. A recent observation at 1.4 GHz using the Parkes radio telescope places an upper limit on a coherent signal of $L_{1400} \lesssim 3 \text{ mJy kpc}^2$, comparable to many faint pulsars but 10 times higher than that of the faintest detected (Camilo et al., in preparation). We also tested archival X-ray data, in particular a relatively long (25 ks), continuous *ROSAT* PSPC observation obtained on 1991 September 28. Given the background rates at the pulsar position, even if PSR J1852+0040 were 100% pulsed, the effective pulsed fraction in the *ROSAT* observation would be no greater than $f_p \approx 27\%$. However, the data are not sensitive enough to reveal it. Similarly, in two available *ASCA* observations, one a dedicated 37 ks observation of Kes 79, and the other a short (9 ks) Galactic ridge survey field observation, the expected pulsar signal is masked by SNR emission because of the $1'$ mirror resolution.

4. SPECTRAL ANALYSIS

Source and background spectra from each data set were accumulated in apertures described in §2. For each observation, data from the two EPIC MOS cameras (MOS1+MOS2) were combined and analyzed as a single data set. After verifying that there were no emission-line features detectable, all spectra were grouped into bins containing a minimum of 40 counts (including background). EPIC pn and EPIC MOS spectra pairs from each observation were fitted simultaneously using the XSPEC package, with the normalization for each data free to vary independently. This allowed for differences in the overall flux calibration, apparent at the $\lesssim 10\%$ level. Some instrumental variation is possibly due to the effects of the distinct pixel size and mirror point-spread

TABLE 2
XMM-Newton SPECTRAL RESULTS FOR PSR J1852+0040

Parameter	2004 Oct 18	2004 Oct 23	Sum
Blackbody Model			
N_{H} (10^{22} cm $^{-2}$)	$1.5^{+0.5}_{-0.4}$	$1.4^{+0.4}_{-0.3}$	$1.5^{+0.3}_{-0.3}$
kT (keV)	$0.43^{+0.04}_{-0.04}$	$0.44^{+0.04}_{-0.03}$	$0.43^{+0.03}_{-0.03}$
pn BB Area (cm 2)	1.0×10^{11}	1.0×10^{11}	1.0×10^{11}
pn BB Flux	1.9×10^{-13}	2.1×10^{-13}	2.0×10^{-13}
pn $L_{\text{BB}}(\text{bol})^{\text{a}}$	3.6×10^{33}	3.5×10^{33}	3.6×10^{33}
MOS BB Area (cm 2)	1.1×10^{11}	1.0×10^{11}	1.0×10^{11}
MOS BB Flux	2.1×10^{-13}	2.2×10^{-13}	2.1×10^{-13}
MOS $L_{\text{BB}}(\text{bol})^{\text{a}}$	4.0×10^{33}	3.7×10^{33}	3.8×10^{33}
$\chi^2_{\nu}(\text{dof})$	0.9(101)	0.7(103)	0.9(132)
Power-law Model			
N_{H} (10^{22} cm $^{-2}$)	$3.4^{+0.8}_{-0.7}$	$3.4^{+0.8}_{-0.7}$	$3.4^{+0.6}_{-0.5}$
Γ	$5.2^{+0.8}_{-0.8}$	$5.2^{+0.7}_{-0.6}$	$5.3^{+0.5}_{-0.5}$
pn PL Flux	2.0×10^{-13}	2.1×10^{-13}	2.0×10^{-13}
pn L_{PL}	1.5×10^{33}	1.6×10^{33}	1.7×10^{33}
MOS PL Flux	2.1×10^{-13}	2.2×10^{-13}	2.1×10^{-13}
MOS L_{PL}	1.6×10^{33}	1.7×10^{33}	1.8×10^{33}
$\chi^2_{\nu}(\text{dof})$	0.8(101)	0.7(103)	0.9(132)

NOTE. — Parameters are derived from a linked fit to the EPIC pn and MOS spectra, with the normalizations independent. Uncertainties are 95% confidence intervals for two interesting parameters. All fluxes are absorbed and given in units of ergs cm $^{-2}$ s $^{-1}$; fluxes are fitted and computed in the 1–5 keV energy band. Luminosities are unabsorbed, in units of ergs s $^{-1}$, and derived for a distance $d = 7.1$ kpc.

^aBolometric blackbody luminosity.

function on measuring the diffuse SNR emission over the source and background regions.

The results of these fits using either an absorbed power-law or blackbody model are presented in Table 2. An acceptable χ^2 statistic is obtained using either model, for each epoch and for the combined data. However, the blackbody model is preferred over the power-law model based on its derived column density of $N_{\text{H}} = (1.5 \pm 0.2) \times 10^{22}$ cm $^{-2}$, which is consistent with that found for the remnant ($N_{\text{H}} \approx 1.6 \times 10^{22}$ cm $^{-2}$, Sun et al. 2004). The fitted column density for the power-law model, $N_{\text{H}} = 3.4^{+0.6}_{-0.5} \times 10^{22}$ cm $^{-2}$, is significantly larger than the integrated 21 cm Galactic value of 2×10^{22} cm $^{-2}$ averaged over a 0.7×0.7 patch of the sky (Dickey & Lockman 1990). The best fitted blackbody model yielded a temperature of $kT_{\text{BB}} = 0.44 \pm 0.03$ keV with a fit statistic of $\chi^2_{\nu} = 0.9$ for 133 degrees of freedom (see Fig. 3). The bolometric luminosity at 7.1 kpc is $L_{\text{BB}}(\text{bol}) = 3.7 \times 10^{33}$ ergs s $^{-1}$, corresponding to a blackbody area of $\approx 1.0 \times 10^{11} d_{7.1}^2$ cm 2 or $\approx 0.5\%$ of the NS surface (see Table 3). The addition of a second component to either spectral model is unconstrained. Evidently the flux has remained steady between both XMM-Newton observations and the Chandra one (Seward et al. 2003) in 2001.

Since the spectral fit to the blackbody model implies that only a small fraction of the NS surface is detected, we also derived an independent upper limit to the effective blackbody temperature of the entire NS surface. Assuming $d = 7.1$ kpc, $N_{\text{H}} = 1.5 \times 10^{22}$ cm $^{-2}$, and a radius at infinity of 12 km, we compared simulated spectra

TABLE 3
ADOPTED SPECTRAL MODEL FOR PSR J1852+0040

Parameter	Value
N_{H} (cm $^{-2}$)	$(1.5 \pm 0.3) \times 10^{22}$
kT (keV)	0.44 ± 0.03
Blackbody emitting area A_{BB} (cm 2)	$(1.0 \pm 0.4) \times 10^{11}$
Blackbody radius R_{BB} (km)	0.9 ± 0.2
Absorbed 1.0–5.0 keV flux (ergs cm $^{-2}$ s $^{-1}$)	$(2.1 \pm 0.1) \times 10^{-13}$
Bolometric luminosity $L_{\text{BB}}(\text{bol})$ (ergs s $^{-1}$)	$(3.7 \pm 0.9) \times 10^{33}$
$\chi^2_{\nu}(\text{dof})$	0.9(133)

NOTE. — All parameters including the normalization are derived from a linked fit to EPIC pn and MOS spectra using summed data from both observations. Uncertainties are 95% confidence intervals for two interesting parameters. Luminosity derived for a distance $d = 7.1$ kpc.

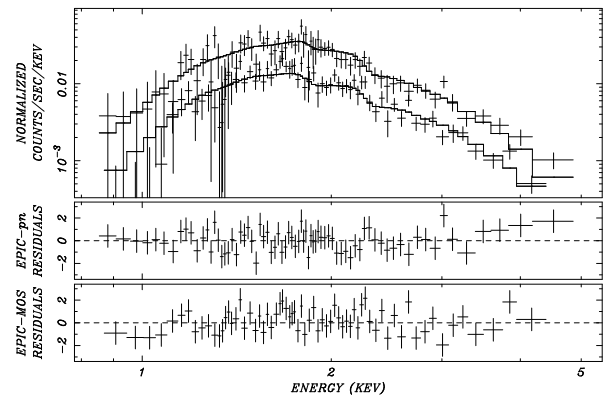


FIG. 3.— The XMM-Newton spectrum of PSR J1852+0040 in Kes 79 from combined observations in 2004 October. *Top panel:* Data from the EPIC pn (*top curve*) and EPIC MOS (*bottom curve*) cameras are shown with the best fitted blackbody model using parameters given in Table 2. *Middle panel:* Residuals to the fit for the EPIC pn. *Bottom panel:* Residuals for the EPIC MOS. The residuals are given in units of sigma.

of increasing blackbody temperature with the data until the predicted spectrum exceeded the observed flux in the lowest energy bins by 3σ . The resulting upper limit is $\log T_e^\infty < 6.24$, which, because of the large distance and column density, is not constraining of NS cooling theory.

Although the blackbody is the preferred spectral model, we note that it is not entirely consistent with the large pulsed fraction of the light curve assumed to be coming from a small spot on the surface of the NS. Light bending caused by the strong gravitational field of the NS generally prevents the observation of such large modulation as is seen from PSR J1852+0040 if the angular dependence of the emitted intensity is isotropic, especially if there are assumed to be two antipodal hot spots. Instead, it is necessary to include beaming due to anisotropic opacity in a strong magnetic field (Zavlin, Shibano, & Pavlov 1995; Özel 2001) in order to reproduce such high pulsed fractions. Such modeling is beyond the scope of this paper. But if the actual pulse shape of PSR J1852+0040 turns out to be variable, as hinted in Figure 2, then it may be necessary to consider an entirely different mechanism, such as cyclotron emission from low-luminosity accretion (Langer & Rappaport 1982). A broad cyclotron spectrum emitted from above

the NS surface may resemble a blackbody in shape while allowing a higher degree of beaming.

5. OPTICAL OBSERVATION

Don Terndrup kindly obtained several CCD images of the field of PSR J1852+0040 using the 2.4 m Hiltner telescope of the MDM Observatory on 2003 July 4 and 5. A thinned, back-illuminated SITe 2048×2048 CCD with a spatial scale of $0.''275$ per $24 \mu\text{m}$ pixel was used with an R -band filter. In Figure 4, we show a combined 60 minute exposure that has seeing of $0.''88$. An astrometric solution for this image was derived in the reference frame of the USNO-A2.0 catalog (Monet et al. 1998) using 65 stars that have an rms dispersion of $0.''49$. The *Chandra* location of PSR J1852+0040 is found to lie $0.''83$ from a star of $R = 20.24$ mag, the latter estimated from the USNO-B1.0 calibration (Monet et al. 2003). Given the distance and extinction to Kes 79 and the upper limit on the spin-down power of the pulsar, we would not expect such a bright star to be its optical counterpart. Neither would we expect to detect the pulsar even at the limiting magnitude of this image, which we estimate as $R = 24.9$. The formal limiting magnitude at the location of the pulsar is somewhat brighter than this because light from the nearby star overlaps part of the $0.''6$ radius *Chandra* error circle.

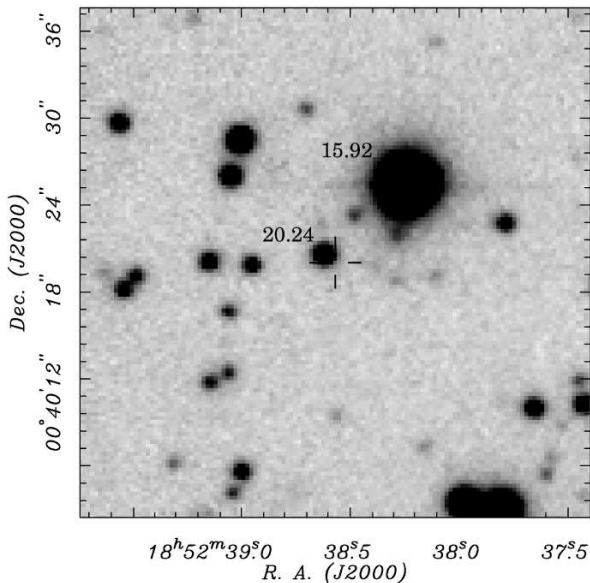


FIG. 4.— R -band CCD image at the location of PSR J1852+0040 in Kes 79 obtained with the 2.4m Hiltner telescope. Seeing is $0.''88$. The tic marks indicate the *Chandra* position of PSR J1852+0040, $18^{\text{h}}52^{\text{m}}38^{\text{s}}.57, +00^{\circ}40'19.''8$ (J2000.0). The magnitude $R = 15.92$ of the bright star is from the USNO-B1.0 catalog, while the magnitude $R = 20.24$ of the fainter star $0.''83$ from the pulsar is scaled from the bright star. The limiting (3σ) magnitude of this image is $R = 24.9$.

6. INTERPRETATION

Using the limited information that we have about PSR J1852+0040 we can begin to evaluate possible models for its X-ray properties, and the implications for the origin of CCOs in general. In this section we explore physical scenarios that are commonly considered for those NSs that are not readily classified, and conclude that none stands out as a preferred explanation of PSR J1852+0040.

6.1. Rotation-Powered Pulsar

Based on its period and spin-derived parameters, the conventional interpretation of PSR J1852+0040 is a rotation-powered pulsar. Its X-ray luminosity is less than the inferred upper limit on its spin-down power, and it is within the typical range for rotation-powered pulsars, $10^{-4} < L_x/\dot{E} < 10^{-2}$ (Possenti et al. 2002). But if L_x/\dot{E} of PSR J1852+0040 is found to be substantially larger than 10^{-2} , that would be unusual, and it would require a larger spin-down age, at odds with the SNR association unless the pulsar were born with nearly its current period. The lower limit on the spin-down age is already greater than the dynamical estimate of the SNR age (5.4–7.5 kyr, Sun et al. 2004). If we adopt $\tau_{\text{SNR}} < 7.5$ kyr as an upper limit to the true age of the pulsar, then the dipole spin-down formula requires a birth period $P_0 > 86$ ms and an initial spin-down power $\dot{E}_0 < 5 \times 10^{36}$ ergs s^{-1} .

PSR J1852+0040 is clearly not among the energetic rotation-powered pulsars, which we define as having $\dot{E} > E_c \approx 4 \times 10^{36}$ erg s^{-1} . All pulsars with $\dot{E} > E_c$ manifest bright wind nebulae and have power-law-dominated spectra with photon indices in the range $0.6 < \Gamma \lesssim 2.1$ (Gotthelf 2004). Pulsars just below E_c are found to have weak wind nebulae, if at all, relative to the pulsar emission. On average, their nebulae are an order-of-magnitude less luminous than their super-critical relatives, and their spectra are not yet well constrained. There is no indication of any hard extended emission around PSR J1852+0040, but deep *Chandra* imaging is needed to exclude a weak nebula. For less energetic rotation-powered pulsars, the interpretation of their X-ray spectra is not as clear because of the diversity of properties of these objects. Measurements of the brighter ones like PSR J1709–4429 (Gotthelf, Halpern, & Dodson 2002; McGowan et al. 2004), which is somewhat less luminous than PSR J1852+0040, suggest a two-component spectrum composed of a blackbody model with temperature $kT_{\text{BB}} \approx 0.15$ keV in addition to harder emission from a power-law model. The temperature and luminosity of PSR J1852+0040 are greater than those of middle-aged pulsars, which have $L_x \sim 10^{31-32.5}$ ergs s^{-1} and $kT_{\text{BB}} \leq 0.15$ keV. The spectra of older pulsars tend to be dominated by even cooler blackbodies (see De Luca et al. 2004). Thus, there is no single category of rotation-powered pulsar into which PSR J1852+0040 fits neatly.

The emission of many intermediate-aged pulsars is dominated by high-energy γ -rays, probably even those not yet detected because of the limited sensitivity of EGRET. The spin parameters of PSR J1852+0040 are not inconsistent with those of known γ -ray pulsars. However, its location is confused with the EGRET source 3EG J1856+0114 that is about 1° from Kes 79, and is coincident with the supernova remnant W44. This EGRET source is hard but variable (Nolan et al. 2003). We can assume that the flux of 3EG J1856+0114, $\approx 3.6 \times 10^{-10}$ ergs $\text{cm}^{-2} \text{s}^{-1}$, is a conservative upper limit on the gamma-ray flux of PSR J1852+0040. Since the upper limit on the spin-down flux $\dot{E}/4\pi d^2$ of PSR J1852+0040 is 4×10^{-10} ergs $\text{cm}^{-2} \text{s}^{-1}$, it could be an as-yet undetected γ -ray pulsar with an efficiency of a few percent, typical of young or middle-aged pulsars.

Even though the X-ray luminosity of PSR J1852+0040 is consistent with minimal NS cooling curves for an age of 10^{3-4} yr (Page et al. 2004), its blackbody temperature implies an emitting area that is just $\approx 0.5\%$ of the NS surface. This is consistent with the highly modulated pulse profile coming from a small rotating hot spot whose measured temperature falls well above any reasonable NS cooling curve. The most likely region for localized heating of the NS surface is at the magnetic poles. The canonical area for the polar cap is $A_{pc} = 2\pi^2 R^3 / Pc \approx 1 \times 10^{10}$ cm². This is only 10% of the area implied by the fit to the X-ray spectrum using the blackbody model. In the outer-gap model for γ -ray pulsars (Wang et al. 1998), the X-ray luminosity of the hot polar cap is limited by the Goldreich-Julian e^\pm current flow of $\dot{N}_0 \approx 2 \times 10^{32} (P/0.105 \text{ s})^{-2} (B/10^{12} \text{ G}) \text{ s}^{-1}$ depositing an average energy per particle of $E_f \approx 4.3$ ergs. The maximum luminosity is $L(\text{bol}) \approx f E_f \dot{N}_0 < 4 \times 10^{32}$ ergs s⁻¹. Here the fraction f of the current reaching the surface is set to 1/2, the maximum possible estimated for a γ -ray pulsar near its death line. While falling short of the observed X-ray luminosity of PSR J1852+0040 by an order-of-magnitude, this prediction applies only to a maximally efficient γ -ray pulsar. Either the γ -ray efficiency or the B_p field is likely to be lower, so this mechanism is hard pressed to account for the X-ray luminosity of PSR J1852+0040. Polar-cap heating models of Harding & Muslimov (2001, 2002) predict even less X-ray luminosity than Wang et al. (1998). Taken at face value, all such models fall short of predicting the apparent area, temperature, and luminosity of the X-ray emission from PSR J1852+0040.

6.2. Anomalous X-ray Pulsar

While the temperature and luminosity of PSR J1852+0040 are greater than those of middle-aged pulsars, its luminosity is less than those of AXPs, which have $L_x \sim 10^{34-35.5}$ ergs s⁻¹ and thermal spectral components of $kT_{\text{BB}} \gtrsim 0.4$ keV (Mereghetti 2002). The spectrum of PSR J1852+0040 is suggestive of a magnetar of low X-ray luminosity, perhaps like the quiescent state of the transient AXP XTE J1810-197 (Halpern & Gotthelf 2005). According to the magnetar theory, the X-ray emission ultimately derives from the decay of an enormous magnetic field ($B \gtrsim 4.4 \times 10^{13}$ G; Duncan & Thompson 1996). Although PSR J1852+0040 could be an ‘‘anomalous,’’ fast AXP, the implied magnetic field strength is insufficient to power the observed X-ray luminosity over the lifetime of the pulsar, estimated as $L_x \tau_{\text{SNR}} \sim 8 \times 10^{44}$ ergs, since the available magnetic energy is only $\approx B^2 R^3 / 6 = 3 \times 10^{43} (B/10^{13})^2$ ergs. More detailed predictions invoking the magnetar theory (e.g., currents on twisted magnetic field lines external to the star; Thompson, Lyutikov, & Kulkarni 2002) are similarly insufficient to sustain the observed X-ray emission.

6.3. Accreting Binary

Although binary NS X-ray transients in quiescence often have luminosities similar to that of PSR J1852+0040, their spectra, as summarized, e.g., by Tomsick et al. (2004), are characterized as softer blackbodies covering the full NS surface, rather than a small hot spot. Even

if the hotter emission from PSR J1852+0040 is hypothesized to come from residual accretion, the current observations disfavor a binary scenario based on its steady long-term flux, lack of orbital Doppler delay, and absence of characteristic red noise in its timing spectrum. The unclassified star $< 1''$ from the *Chandra* position, while unlikely to be a binary companion of PSR J1852+0040, prevents us from deriving a constraining upper limit on optical emission from either the pulsar itself or a fall-back accretion disk.

6.4. Fall-back Accretion

Even if PSR J1852+0040 possesses a fossil accretion disk, it may be unable to accrete because the magnetospheric radius is $r_m = 3 \times 10^8 \mu_{30}^{4/7} (M/M_\odot)^{1/7} L_{37}^{-2/7} R_6^{-2/7}$ cm, which is 3×10^9 cm for an assumed magnetic moment $\mu = B_p R^3 / 2 \approx 10^{30}$ G cm³ and an observed $L = GM\dot{m}/R = 3.7 \times 10^{33}$ ergs s⁻¹. Therefore, the magnetic dipole pressure ejects any potential accreting matter well outside the light cylinder radius, $r_\ell = cP/2\pi = 5 \times 10^8$ cm. Only in the case of B_p as small as 7×10^8 G could PSR J1852+0040 be a ‘‘slow rotator,’’ with $P \approx P_{\text{eq}}$, since the equilibrium (or minimum) period for disk accretion is $P_{\text{eq}} = 3.6 \mu_{30}^{6/7} (M/M_\odot)^{-2/7} L_{37}^{-3/7} R_6^{-3/7}$ s. While such a value of B_p is common among low-mass X-ray binaries, it would be surprising for such a young NS.

For an intermediate value of the magnetic field strength, PSR J1852+0040 could be in the propeller regime, $P < P_{\text{eq}}$, in which matter is flung out from the magnetospheric radius at a rate \dot{m} , which causes it to spin down at a rate $\dot{P} \approx 2 \dot{m} r_m^2 I^{-1} P (1 - P/P_{\text{eq}})$ (e.g., Menou et al. 1999; Zavlin et al. 2004), where $I \approx 10^{45}$ g cm² is the NS moment of inertia. The observed upper limit $\dot{P} < 7 \times 10^{-14}$ s s⁻¹ sets an upper limit of $\dot{m} < 3.7 \times 10^{16} (r_m/10^8 \text{ cm})^{-2}$ g s⁻¹ in the propeller scenario. But in that case, it is not clear how the highly pulsed, thermal X-ray emission is produced. Even if the bulk of the fall-back material is ejected, as little as 3×10^{13} g s⁻¹ accreting onto the NS surface is sufficient to account for the observed luminosity. This model was proposed by Alpar (2001) for CCOs in general, with the additional requirement that their weak or undetected pulsations might be washed out by an electron scattering corona accumulated from the much larger \dot{m} at the propeller radius. Now, of course, this caveat no longer applies in the case of PSR J1852+0040. Indeed, the nearly 100% modulation of its pulsed light curve in the first observation requires that the propeller mechanism create no significant X-ray emission or X-ray scattering screen at the magnetospheric boundary. As long as an accretion scenario is being considered, there remains the associated possibility that the X-rays are *not* surface thermal emission, but a broad cyclotron feature that corresponds to a range of magnetic field strengths $B < 10^{12}$ G just above the surface.

Because of the large distance and interstellar extinction to PSR J1852+0040, our optical observation does not yet rule out the presence of a fossil accretion disk. We computed the optical emission of a standard blackbody disk that is terminated at inner radius $r_{\text{in}} = r_m$ and having values of \dot{m} allowed in the propeller scenario for PSR J1852+0040. These important parameters must satisfy

the criterion $\dot{m} r_{\text{in}}^2 < 3.7 \times 10^{32} \text{ g s}^{-1} \text{ cm}^2$ derived in the previous paragraph. We include an extinction of 6.8 mag in the R -band, corresponding to $N_{\text{H}} = 1.5 \times 10^{22} \text{ cm}^{-2}$. We find that face-on disks with $r_{\text{in}} > 5 \times 10^7 \text{ cm}$, an order of magnitude smaller than the light cylinder radius, have $R > 25 \text{ mag}$, which is fainter than our optical limit. As long as there are significant difficulties in understanding the temperature and (possibly variable) modulation of the pulsed emission in the context of an isolated NS, accretion from a fall-back disk remains a viable option for PSR J1852+0040.

6.5. Comparison with PSR J1210–5226

Apparently, the Griffin-like properties of PSR J1852+0040 are typical only of the CCOs, and are not easily accounted for in any one theoretical framework. Detailed comparison is possible only with PSR J1210–5226, the 424 ms pulsar in PKS 1209–51/52 that has similar luminosity but is modulated with a pulsed fraction of only $\approx 10\%$ (Zavlin et al. 2000). Although still classified as a CCO, the complex spin-down behavior and spectrum of PSR J1210–5226 set it apart from any other isolated NS. Whether it is unique or a typical CCO is not yet clear. Its flux is found to be steady, but large variations of its period derivative may imply a wide binary system ($P_{\text{orb}} \sim 0.2 - 6 \text{ yr}$), frequent large glitches, or accretion from fall-back material (Zavlin et al. 2004). In any case, its wildly varying spin-down age is inconsistent with the remnant age of $\sim 10 \text{ kyr}$. The X-ray spectrum shows broad absorption features at 0.7 and 1.4 keV (Sanwal et al. 2002) and possibly at 2.1 and 2.8 keV when fitted with a thermal blackbody continuum model of $kT_{\text{BB}} \approx 0.21 \text{ keV}$ and hard tail of $kT_{\text{BB}} \approx 0.40 \text{ keV}$ (Bignami et al. 2003). If PSR J1852+0040 is like PSR J1210–5226, we would expect to see similar spectral features and timing behavior; the limited data in hand are not strongly constraining.

7. CONCLUSIONS AND FUTURE WORK

PSR J1852+0040 is clearly a young NS associated with Kes 79, and apparently not a close binary. As a rotation-

powered pulsar, the inferred upper limit on its spin-down power is consistent with the absence of a bright pulsar wind nebula. From the age discrepancy between the pulsar and SNR, it is possible that the initial spin-down power of PSR J1852+0040 is sub-critical ($\dot{E}_0 < \dot{E}_c$); this may prove to be a defining property of the CCOs. What is clearly distinctive about PSR J1852+0040 is its hot thermal emission and relatively high luminosity (for its age and \dot{E}). These factors, along with the large pulse modulation, suggest a rotating hot spot, but the area and luminosity of this spot are greater by an order-of-magnitude than can be explained by existing theories of isolated neutron stars. Accretion of fall-back material from a fossil disk in the propeller regime remains an option. An alternative interpretation is a low-luminosity AXP, but the inferred magnetic field and rotation period are smaller than expected in this scenario. The X-rays from the pulsar are not easily produced in the context of the magnetar theory as the inferred B field is insufficient to power the observed emission over the implied age of the NS. These unexplained X-ray properties of PSR J1852+0040 may be symptomatic of the entire class of CCOs, and may require intensive observational and theoretical efforts to understand. A radio detection would demonstrate cleanly that PSR J1852+0040 is a rotation-powered pulsar, but the absence of radio pulsations would be inconclusive. Frequent X-ray monitoring will test for evidence of accretion torques and/or glitches, and establish whether the X-ray flux and pulse profile are variable. By analogy with other isolated neutron stars that have broad X-ray absorption features, a deeper spectral study of PSR J1852+0040 may prove to be revealing.

This investigation is based on observations obtained with *XMM-Newton*, an ESA science mission with instruments and contributions directly funded by ESA Member States and NASA. We thank Don Terndrup for obtaining the optical image used in Figure 4. This work is supported by NASA XMM grant NNG05GD46G.

REFERENCES

- Alpar, M. A. 2001, *ApJ*, 554, 1245
 Baade, W., & Zwicky, F. 1934, *Phys. Rev.* 45, 138
 Bignami, G. F., Caraveo, P. A., De Luca, A., & Mereghetti, S. 2003 *Nature*, 423, 725
 Buccheri, R., et al. 1983, *A&A*, 128, 245
 Chakrabarty, D., Pivovarov, M. J., Hernquist, L. E., Heyl, J. S., & Narayan, R. 2001, *ApJ*, 548, 800
 Caraveo, P. A., Bignami, G. F., & Trümper, J. E. 1996, *A&A Rev.*, 7, 209
 Case, G. L., & Bhattacharya, D. 1998 *ApJ*, 504, 761
 De Luca, A., Mereghetti, S., Caraveo, P. A., Moroni, M., Mignani, R. P., & Bignami, G. F. 2004, *A&A*, 418, 625
 Dickey, J. M., & Lockman, F. J. 1990, *ARA&A*, 28, 215
 Duncan, R. C., & Thompson, C. 1992, *ApJ*, 392, 9
 ———. 1996, in *High Velocity Neutron Stars*, AIP Conf. Proc. 366, ed. R. E. Rothschild & R. E. Lingefelner (New York: AIP), 111
 Frail, D. A., & Clifton, T. R. 1989, *ApJ*, 336, 854
 Gorham, P. W., Ray, P. S., Anderson, S. B., Kulkarni, S. R., & Prince, T. A. 1996, *ApJ*, 458, 257
 Gotthelf, E. V. 2004, in *Young Neutron Stars and their Environments*, IAU Symp. 218, ed. F. Camilo & B. M. Gaensler (San Francisco: ASP), 225
 Gotthelf, E. V., Halpern, J. P., & Dodson, R. 2002, *ApJ*, 567, L125
 Gotthelf, E. V., Vasisht, G., Dotani, T. 1999, *ApJ*, 522, L49
 Green, D. A., & Dewdney, P. E. 1992, *MNRAS*, 254, 686
 Halpern, J. P., & Gotthelf, E. V. 2005, *ApJ*, 618, 874
 Harding, A. K., & Muslimov, A. G. 2001, *ApJ*, 556, 987
 ———. 2002, *ApJ*, 568, 862
 Helfand, D. J., & Becker, R. H. 1984, *Nature*, 307, 215
 Langer, S. H., & Rappaport, S. A. 1982, *ApJ*, 257, 733
 McGowan, K. E., Zane, S., Cropper, M., Kennea, J. A., Córdova, F. A., Ho, C., Sasseen, T., & Vestrand, W. T. 2004, *ApJ*, 600, 343
 Menou, K., Esin, A. A., Narayan, R., Garcia, M. R., Lasota, J.-P., & McClintock, J. E. 2001, *ApJ*, 520, 276
 Mereghetti, S., Israel, G. L., & Stella, L. 1998, *MNRAS*, 296, 689
 Mereghetti, S. 2002, in *Proc. 270 WE-Heraeus Seminar, Neutron Stars, Pulsars, and Supernova Remnants*, ed. W. Becker, H. Lesch, & J. Trümper (MPE Rep. 278; Garching: MPE), 29
 Monet, D., et al. 1998, *USNO-SA2.0* (Washington, DC: US Naval Obs.)
 ———. 2003, *AJ*, 125, 984
 Nolan, P. L., Tompkins, W. F., Grenier, I. A., & Michelson, P. F. 2003, *ApJ*, 597, 615
 Özel, F. 2001, *ApJ*, 563, 276
 Page, D., Lattimer, J., Prakash, M., & Steiner, A. W. 2004, *ApJS*, 155, 623
 Pavlov, G. G., Sanwal, D., & Teter, M. A. 2004, in *Young Neutron Stars and their Environment*, IAU Symp. 218, ed. F. Camilo & B. M. Gaensler (San Francisco: ASP), 239
 Pavlov, G. G., Zavlin, Sanwal, D., & Trümper, J. 2002, *ApJ*, 569, L95
 Pavlov, G. G., Zavlin, & Trümper, J. 1999, *ApJ*, 511, L45
 Petre, R., Becker, C. M., & Winkler, P. F. 1982, *ApJ*, 440, 706

- Possenti, A., Cerutti, R., Colpi, M., & Mereghetti, S. 2002, *A&A*, 387, 993
- Sanwal, D., Pavlov, G. G., Zavlin, V. E., & Teter, M. A. 2002, *ApJ*, 574, 61
- Seward, F. D., Slane, P. O., Smith, R. K., & Sun, M. 2003, *ApJ*, 584, 414
- Seward, F. D., & Velusamy, T. 1995, *ApJ*, 439, 715
- Slane, P., Gaensler, B. M., Dame, T. M., Hughes, J. P., Plucinsky, P. P., & Green, A. 1999, *ApJ*, 525, 357
- Slane, P., Hughes, J. P., Edgar, R. J., Plucinsky, P. P., Miyata, E., Tsunemi, H., & Aschenbach, B. 2001, *ApJ*, 548, 814
- Sun, M., Seward, F. D., Smith, R. K., & Slane, P. O. 2004, *ApJ*, 605, 742
- Tananbaum, H. 1999, *IAU Circ.* 7246
- Thompson, C., Lyutikov, M., & Kulkarni, S. R. 2002, *ApJ*, 574, 332
- Tomsick, J. A., Gelino, D. M., Halpern, J. P., & Kaaret, P. 2004, *ApJ*, 610, 933
- Turner, M. J. L., Briel, U. G., Ferrando, P., Griffiths, R. G., & Villa, G. E. 2003, *SPIE*, 4851, 169
- Wang, F. Y.-H., Ruderman, M., Halpern, J. P., & Zhu, T. 1998, *ApJ*, 498, 373
- Zavlin, V. E., Pavlov, G. G., & Sanwal, D. 2004, *ApJ*, 606, 444
- Zavlin, V. E., Pavlov, G. G., Sanwal, D., & Trümper, J. 2000, *ApJ*, 540, L25
- Zavlin, V. E., Shibanov, Y. A., & Pavlov, G. G. 1995, *Astronomy Letters*, 21, 149